# Magnetic, $^{57}$Fe Mössbauer, and IR Monitoring of the Thermal Spin Transition in a New Family of Iron(II) Spin-Transition Complexes

**Arno F. Stassen,[a] Matthias Grunert,[b] Eva Dova,[c] Martin Müller,[d] Peter Weinberger,[d] Günter Wiesinger,[d] Henk Schenk,[c] Wolfgang Linert,[b] Jaap G. Haasnoot,*[a] and Jan Reedijk[a]**

**Keywords:** Spin crossover / Iron / Tetrazole ligand / Mössbauer spectroscopy / Variable-temperature IR spectroscopy

A new family of iron(II) tetrafluoroborate and perchlorate spin-crossover compounds has been synthesised and is discussed. The iron(II) ion is surrounded by six 1-ethyltetrazole ligands, which are halogen-substituted on the C2 atom of the ethyl group. The spin-crossover temperatures $T_{1/2}$ are high compared to the unsubstituted (1-alkyltetrazole)iron(II) complexes. The shape of the spin-transition curve (i.e. $\gamma_{HS}$ vs. $T$) varies largely over the different complexes and appears to be influenced neither by the crystal packing, nor by the electronic effects. The temperature-dependent spin-transition behaviour has been studied by magnetic susceptibility and by $^{57}$Fe-Mössbauer spectroscopy. These data have been supported by temperature-dependent mid-range infrared spectroscopy: the thermally induced spin transition has been observed by direct monitoring of the aromatic C–H stretching frequency.


## Introduction

Among compounds featuring temperature-dependent spin transitions, the [Fe(1-alkyltetrazole)$_6$](anion)$_2$ compounds are probably the most studied complexes.[1−4] Methyl-, ethyl-, propyl- and isopropyltetrazole (*mtz*, *etz*, *ptz* and *iptz*) were used as ligands for iron(II) spin-crossover complexes[2] as early as 1982 by Franke et al. These complexes are special for several reasons, they were the first reported members of a family of spin-crossover complexes with monodentate ligands showing a strong cooperativity,[5] which led to the development of the model of the elastic interactions.[6] The synthesis of both the ligands and the complexes is straightforward and these iron(II) complexes are very stable compared to other iron(II) spin-crossover complexes. Finally, the spin-crossover behaviour among these four almost identical complexes differs strongly: the spin transition depends both on the ligand,[2] and the anion.[1,2,7]

Recently, the spin-crossover behaviour of a series of iron(II) complexes containing the new ligand 1-(2-chloroethyl)tetrazole (*teec*) was published.[8] These complexes show, depending on the anion and applied synthetic method, a wide variety of magnetic behaviour including transitions in two steps, residues of high-spin species at low temperature and a thermal hysteresis effect.

In order to study the influence of the size of the halogen atom in the 1-(2-haloethyl)tetrazole spin-crossover complexes, now also the fluorine- (*teef*), bromine- (*teeb*) and iodine-substituted (*teei*) ligands have also been synthesised. From donor-number calculations[9] and NMR spectroscopy[10] it is known that the electronic influence of the halogen atom on the electron density of the tetrazole ring is negligible. Therefore, the changes in ligand-field strength (and subsequently differences in spin-transition temperature $T_{1/2}$) should almost completely be caused by the crystal packing and not by electronic effects.

The ligands *teef*, *teeb* and *teei* have been used to synthesise iron(II) tetrafluoroborate and perchlorate complexes. The magnetic and spectral properties of these complexes have been studied to observe the influence of the ligand size on the thermal spin transition. Because of the potential explosive nature of perchlorate compounds, no Mössbauer or infrared measurements have been performed on the perchlorate complexes.

[a] Leiden Institute of Chemistry, Gorlaeus Laboratories, Leiden University,
P. O. Box 9502, 2300 RA Leiden, The Netherlands
Fax: (internat.) + 31-71/527-4671
E-mail: haasnoot@chem.leidenuniv.nl
[b] Institute of Applied Synthetic Chemistry, Vienna University of Technology,
Getreidemarkt 9/163-AC, 1060 Vienna, Austria
[c] Institute of Molecular Chemistry, Laboratory of Crystallography, Universiteit van Amsterdam,
Nieuwe Achtergracht 166, 1018WV Amsterdam, The Netherlands
[d] Institute of Solid State Physics, Vienna University of Technology,
Hauptstrasse 8-10/131, 1040 Vienna, Austria

## Results and Discussion

### IR Spectroscopy of the Ligands

Mid-range FT-IR spectra of the undiluted complexes, and the ligands as KBr pellets have been recorded within the range of 4400−450 $cm^{-1}$ at room temperature. For the interpretation of the spectra the observed data were compared with general tables in the compilation of Hesse et al.,[11] several publications of analogous tetrazole compounds,[12−20] as well as with the spectra of the starting products. One of the most prominent absorption features for the tetrazole ring is detected around 3140 $cm^{-1}$ (stretching vibration $\nu_{C-H}$ at the tetrazole ring[12−14]). At about 1485 $cm^{-1}$ the $\nu_{N2=N3}$ stretching vibration[15,16] appears, which also influences the $\nu_{N1=C5}$ as well as the $\nu_{N1=Calkyl}$ stretching vibration. The shifts of most of the bands of the tetrazole ring, caused by substitution of different halogen atoms, are not significant. An exception is the band which shifts due to a heavier halogen substituent from 1107 to 1096 $cm^{-1}$ and belongs to the $\nu_{C5-N1}$ stretching vibration,[14] as well as the in-plane deformation of the C5−H1 bond ($\delta_{C5-H1}$). An in-plane ring vibration[13,14] ($\delta_{ring2}$) shifts in the same manner from 963 to 900 $cm^{-1}$. In the aliphatic part this trend can only be observed for the $\nu_{N1-Calkyl}$[11] stretching band (shift between 1363 and 1353 $cm^{-1}$) and for the deformation of the C−H2 bonds[11] ($\delta_{C-H2}$). Table 1 gives an overview of the changes upon coordination, and lists other important IR bands.

### IR Spectroscopy of the Complexes

In the iron(II) tetrafluoroborate complexes, two deformation vibrations[21] ($\delta_{B-F}$) belonging to the tetrafluoroborate are identified. The only clearly visible, non-overlapping, deformation vibrations are at 533 and 522 $cm^{-1}$ in the case of *teef*, *teec* and *teeb*, whereas in the compound with *teei* as ligand, a band at 515 $cm^{-1}$ with a shoulder at 522 $cm^{-1}$ appears. The B−F stretching vibration ($\nu_{B-F}$) is responsible for the broad background between 1600 and 800 $cm^{-1}$. The maximum is located at about 1060 $cm^{-1}$.

Vibrations in the spectra measured at room temperature for the pure ligands and the iron(II) tetrafluoroborate complexes show differences of about −3 and +70 $cm^{-1}$, respectively. Interestingly, these shifts show different sensitivity: shifts of the aromatic and aliphatic C−H stretching differ between pure ligand and complex, e.g. $\nu_{C5-H}$ (between +1 and +9 $cm^{-1}$), $\delta_{C-H2}$ (between 0 and +19 $cm^{-1}$) and the broad aromatic overtone band (+33 to +67$cm^{-1}$). No strong influence is observed on these bands due to the variation of the halogen substituent. However, the bands associated with the tetrazole ring vibrations are influenced by the halogen substituent. With increasing halogen mass, the difference in frequency between the bands observed in the pure ligand and the iron(II) complex containing this ligand increases. The stretching vibration $\nu_{N2=N3}$ shifts upon coordination by +16 $cm^{-1}$ for the fluorine-substituted compound, +17 $cm^{-1}$ for the chlorine-, +26 $cm^{-1}$ for the bromine- and +27 $cm^{-1}$ for the iodine-substituted com-

Table 1. Prominent mid IR bands of the (haloethyl)tetrazole ligands investigated; wavenumbers in $cm^{-1}$; ν = stretching, δ = deformation or in-plane vibration of the ring, γ out-of-plane

| Compound | teef | teec | teeb | teei |
|---|---|---|---|---|
| ν(C−H)[12−14] | 3138 s | 3142 s | 3136 s | 3142 s |
| ν(C−H2)[11] | 3003 w | 3031 m | 3040 m | 3027 m |
| | 2972 m | 3009 w | 3005 m | 2999 w |
| | 2909 w | 2974 m | 2976 m | 2961 w |
| | | 2908 m | 2952 w | |
| Aromatic overtone band | 1750 w | 1743 m | 1739 m | 1757 m |
| | 1723 w | | | |
| ν(N2=N3)[13−16] {+ν(C5−N1) + ν($C_{alkyl}$−N1)} | 1487 s | 1486 s | 1481 s | 1485 s |
| δ(C−H2)[11] | 1429 m | 1435 m | 1432 m | 1443 m |
| | 1434 m | 1423 m | 1419 m | 1425 m |
| ν(N1-$C_{alkyl}$)[11] | 1363 m | 1358 m | 1355 m | 1353 m |
| ν(C−F)[11,17,18] | 1263 m | | | |
| δ(ring1)[12−14] | 1246 m | 1255 m | 1265 s | 1263 m |
| ν(C=N4), ν(N1−N2)[14] | 1174 vs | 1176 vs | 1174 vs | 1172 vs |
| ν(C5−N1), δ(C5−H)[14] | 1107 s | 1101 s | 1098 s | 1096 s |
| ν(N3−N4)[12−14] | 1041 s | 1041 m | 1033 m | 1042 w |
| ν(N1−N2)[14] | 973 sh | 971 s | 968 s | 970 s |
| δ(ring2)[13,14] in-plane bending {δ(NCN)} | 963 m | 947 m | 930 m | 900 m |
| γ($H_2C-CH_2$) | 878 sh | 914 s | 892 s | 887 sh |
| | 858 s | 875 s | 872 s | 881 s |
| γ(ring3)[13,14] out-of-plane | 722 m | 721 m | 720 m | 717 w |
| γ(ring4)[13,14] out-of-plane | 679 s | 677 s | 673 vs | 660 vs |
| | | 667 vs | | |
| ν(C−Cl)[18] | | 461 s | | |

  

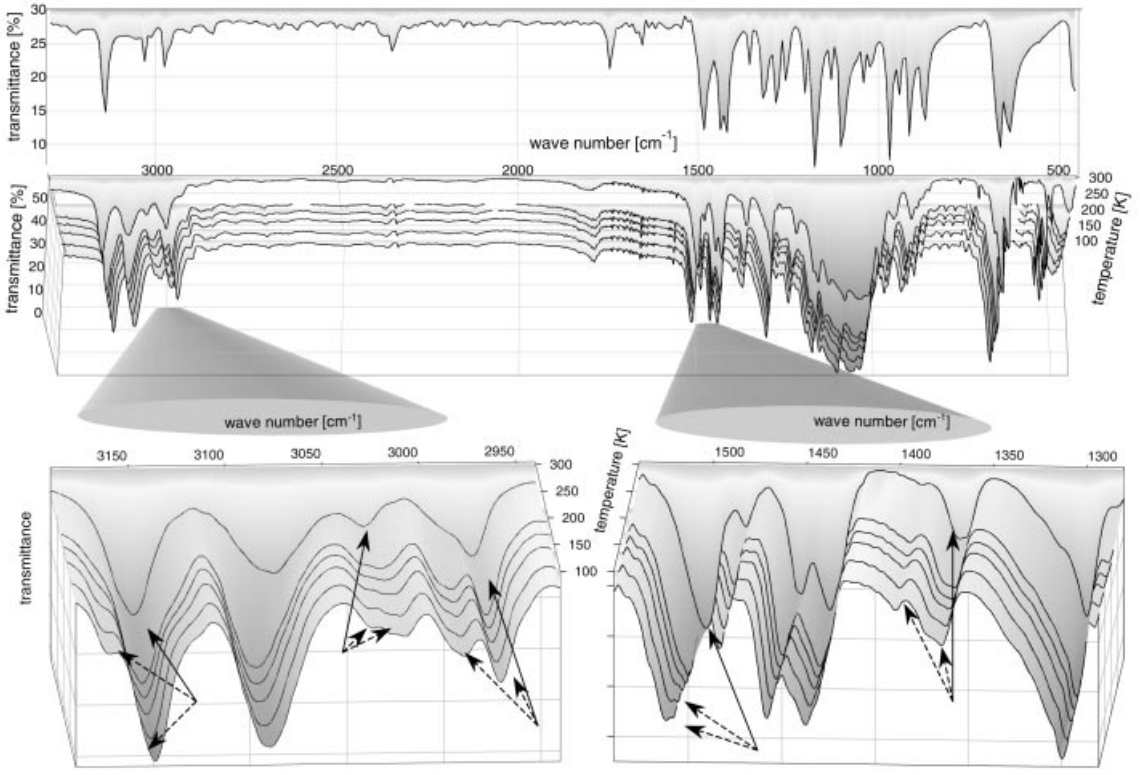


Figure 1. Comparison of the ligand (*teec*) top, with its iron(II) tetrafluoroborate complex, measured at different temperatures between 301 and 100 K (centre); the arrows mark changes of bands in the HS (solid) to a mixed HS−LS state (dashed)

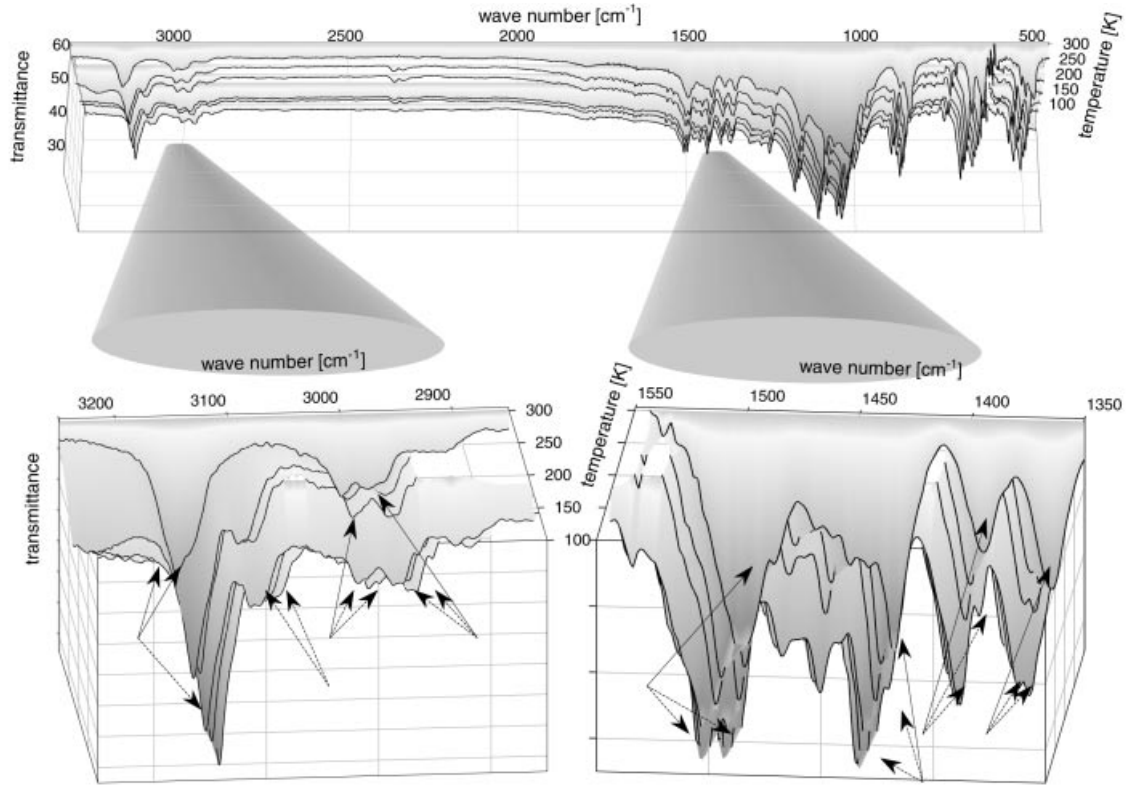


Figure 2. Temperature-dependent infrared spectroscopy of $[Fe(teef)_6](BF_4)_2$; the arrows mark changes of bands in the HS (solid) to a mixed HS−LS state (dashed)

  

pound. The asymmetric out-of-plane ring vibrations around 650 $cm^{-1}$ are not significantly influenced at all. Figure 1 provides an illustration of the changes in the mid-range IR spectrum of the *teec* ligand compared to its iron(II) tetrafluoroborate complex at room temperature in the high-spin state and at 100 K in the low-spin state.

Due to the change of the spin state of iron(II) from LS to HS, the anti-bonding $e_g$-orbitals are populated, thus weakening the Fe−N4 bond. This weakening results in a bond-length expansion[20] of about 5−10%. The expansion can be detected as a shift in the far-infrared region, as has been shown in a similar case.[19] The structural changes around the iron centre also influence bond strengths in the ligand. The stretching vibrations in the tetrazole ring ($\nu_{N2=N3}$) and the C5−H stretching vibration of the tetrazole hydrogen atom (which is located close to the metal centre) are mostly influenced, but the stretching vibrations of the alkyl chain are also slightly affected. The asymmetric ring vibration ($\gamma_{ring2}$, $\gamma_{ring3}$) and the C−H2 deformation of the chain ($\delta_{C-H2}$) are not significantly influenced.

Figure 2 shows that upon cooling, a thermal iron(II) spin transition takes place yielding new small bands. These new bands are associated with the low-spin state. The new stretching vibration $\nu_{C5-H}$, due to the LS species, shifts with larger substituents (F, Cl, Br and I) to higher energies (3101, 3172, 3175 and 3176 $cm^{-1}$). Bands known from the high-spin spectra are also shifted, mainly to higher energies (e.g. $\nu_{C5-H}$ and $\delta_{C-H2}$). A splitting of one of the bands ($\nu_{N2=N3}$) is also observed. This effect has also been detected in the complexes of *teeb* and *teei*.

The vibrational spectrum of $[Fe(teef)_6](BF_4)_2$ shows the shoulder of the $\nu_{C-H}$(HS) band vanishing upon cooling. The newly arising $\nu_{C-H}$(LS) shows a band splitting, which is observed at about 3100 $cm^{-1}$ (see Figure 2). Furthermore, strong band splittings in the low-spin case are observed for the $\nu_{N2=N3}$ vibration, whereas for most of the other stretching vibrations this splitting is not very well pronounced.

Table 2 lists the vibrational frequencies of the iron(II) tetrafluoroborate complexes with *teef*, *teec*, *teeb* and *teei* at room temperature in the high-spin state and at about 100 K. At this temperature, in all four complexes, the majority of the iron(II) ions that undergo a thermal spin transition will be in the low-spin state (Figure 9, A).

Table 2. Mid IR bands of iron(II) $[Fe(L)_6](BF_4)_2$ with L = *teef*, *teec*, *teeb*, *teei* at room temperature and at about 100 K; frequencies in $cm^{-1}$; ν = stretching, δ = deformation or in-plane of the ring, γ = out-of-plane, italic numbers = significant changes during the spin conversion, bold = bands which are only observed in HS or LS state

| Compound | Fe−*teef* (HS) | Fe−*teef* (LS) | Fe−*teec* (HS) | Fe−*teec* (LS) | Fe−*teeb* (HS) | Fe−*teeb* (LS) | Fe−*teei* (HS) | Fe−*teei* (LS) |
|---|---|---|---|---|---|---|---|---|
| ν(C−H)[12−14] | *3145 s/3134 sh* | 3141 s | 3147 s | **3172 sh**/*3148 s* | 3145 s | **3175 sh**/*3149 s* | 3143s | **3176 m**/*3146 s* |
| | | **3101 m/3092** | | | | | | |
| ν(C−H)[11] | 2999 m | *3008 m/2998 m* | 3974 m | 3089 s | 3038 m | *3093 s/3075 sh* | *3026 m/3004 m* | *3021 m/3008 m* |
| | 2975 m | *2974 m/2966 m* | 3028 w | *3036 sh/3020 w* | 3036 w | 3035 w | 2967 m | *2971 m/2963 sh* |
| | | | 2972 m | *2989 m/2970 m* | 2975 m | 2984 m | | |
| | | | | | 2927 sh | 2927 w | | |
| Aromatic overtone band | 1789 w | 1794 w | 1800 w | 1786 m | 1793 w | *1794 w/1781 w* | 1790 m | *1796 m/1774 w* |
| ν(N2=N3)[13−16] {+ ν(C5−N1) + ν($C_{alkyl}$−N1)} | 1503 s | *1505 s/1495 s* | 1503 s | *1512 s/1510 s* | *1507 s/1503 s* | *1511 s/1508 s* | 1508 s | 1514 s |
| δ(C−H2)[11] | 1445 w | 1434 w | 1453 m | 1458 m | 1451 m | 1455 m | 1455 m | 1461 m/1455 m |
| | 1434w | 1426vw | 1437m | 1437m | 1429m | 1431 m/1427 m | 1428 m/1419 m | 1443 m |
| | | | | | | | | 1427 m/1419 m |
| | 1394 w | 1394 w/1385 vw | | | | | | |
| ν(N1−$C_{alkyl}$)[11] | 1364 w | 1368 w/1363 w | 1367 w | 1389 vw/1364 w | 1363 w | 1363 w | 1364 m | 1368 m/1359 m |
| | 1300 vw | 1307 w | 1299 m | 1299 m | 1285 m | 1307 w/1288 m | 1312 w | 1313 w/1304 w |
| | | | | | | | 1287 m/1276 m | 1293 m/1281 m |
| ν(C−F)[11,17,18] | 1265 vw | 1273 w | | | | | | |
| δ(ring1)[12−14] | 1245 w | 1248 w | 1229 w | 1235 w | 1243 w | 1247 w | 1227 m | 1235 m |
| ν(C=N4), ν(N1−N2)[14] | 1174 vs/1164 sh | 1176 m/1163 w | 1172 vs | 1170 vs | 1170 vs | 1170 vs | 1194 s/1175 s | 1198 s/1177 s |
| | | | | | | | 1132 s | 1135 s |
| ν(C5−N1) + δ(C5−H)[14] in-plane | 1106 s | 1108 vs | 1101 vs | 1102 vs | 1097 vs | 1097 vs | 1094 s | 1108 s/1095 s |
| ν(B−F)[21] | 1051 vs | 1052 vs | 1062 vs | 1062 vs | 1059 vs | 1061 vs | 1056 vs | 1055 vs |
| ν(N3−N4)[12−14] | 1039 vs | 1039 vs | 1039 vs | 1039vs | 1040 vs | 1038 vs | 1040 sh | 1046 vs/1040 sh |
| ν(N1−N2)[14] | 994 w | 997 w | 1001 s | | 999 m | | 1019 s/1003 m | 998 m |
| δ(ring2)[13,14] in-plane-banding {δ(NCN)} | 970 vw | 970 vw | 959 w | 961w | 967 vw/946 w | 970 w | 939 m/930 m | 932 m |
| γ($H_2C$−$CH_2$) | 886 w | 884 w | 910 m | 913 m | 880 m | 887 m | 893 w | 897 w/869 w |
| δ(C−H2)[11] | 861m | 971 w/861 m | 878 w | 874 w | 880 m | 887 m | 840 m | 837 m |
| γ(ring3)[13−14] out-of-plane | 721w | 722 w | 721 w | 726 vw | 720 w | 725 vw | 724 w | 719 w |
| γ(ring4)[13−14] out-of-plane | 679 s | 681 s | 666 s | 668 vs | 670 m | 675 m/670 m | 670 m/664 m | 663 m |
| | 648 s | 645 s | 645 m | 653 m | 650 m | 654 m/648 m | 653 m | 647 m |
| | | | | | 571 m | 570 m | | |
| δ(B−F)[21] | 522 m | 521 m | 533 w | 534 w | 533 w | 534 w | 522 sh/515 m | 524 m |
| | 500 m | 502 m | 522 w | 521 w | 521 w | 521 w | | 516 m |
| ν(C−Cl)[18] | | | 473 m | 480 w | | | | |

  

### Mössbauer Spectroscopy

#### *teef*

Representative spectra recorded at ambient and liquid helium temperatures and at a temperature within the spin transition regime are displayed in Figure 3. The substantial reduction of the absorption area due to the decreasing Lamb-Mössbauer factor upon increasing the temperature is obvious from this figure. This reduction indicates a significant weakening of the bond strength at higher temperatures and quite a low Debye temperature. On taking a closer look at the high-spin pattern (see Figure 4), a single doublet is insufficient to fit the data to a reasonable extent. This can only be performed successfully if the presence of two doublets with equal intensity is assumed. Due to the lack of resolution, however, a certain ambiguity remains concerning the exact absorption area, the error being estimated to lie around 10%. On cooling below ambient temperature the onset of the high-spin to low-spin transition can be detected at 160 K by the occurrence of a further subpattern exhibiting a significantly lower isomer shift and an almost collapsed quadrupole splitting (Table 3). Thus, the resolution of the low-spin state pattern is too poor to resolve the two species as observed in the high-spin case. The transition is found to be centred at about 140 K (Figure 5), which is in close agreement with the magnetic susceptibility results (vide infra). It is, however, an incomplete one, as at 4.2 K approximately 44% still remains in the high-spin state. The temperature dependence of the isomer shift (decreasing values on increasing the temperature) is mainly due to the second-order Doppler effect, with only a small contribution remaining from the change of the lattice dimensions depending on the temperature.

#### *teeb*

In the $^{57}$Fe Mössbauer spectra of [Fe(*teeb*)$_6$](BF$_4$)$_2$ (see Figure 6 and Table 4), only one doublet is observed for the high-spin state. The transition to the low-spin state is gradual and complete, starting at about 210 K and being completed at about 110 K. The transition is centred at approximately 160 K, in agreement with the bulk magnetic data.

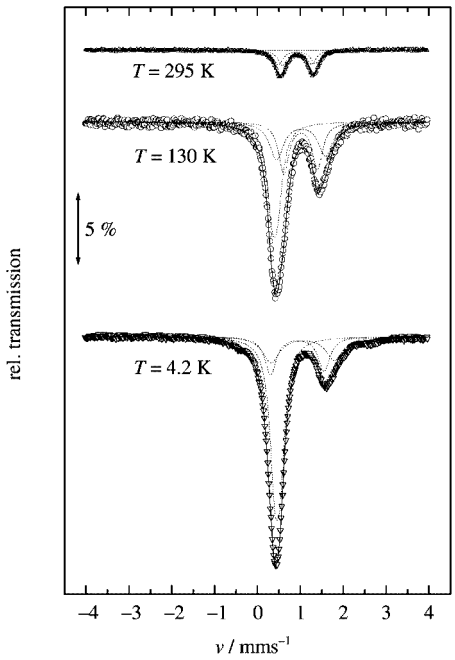


Figure 3. $^{57}$Fe Mössbauer spectra recorded from [Fe(*teef*)$_6$](BF$_4$)$_2$ at different temperatures; triangles and circles are experimental points, solid (broken) lines computer fit described in the text

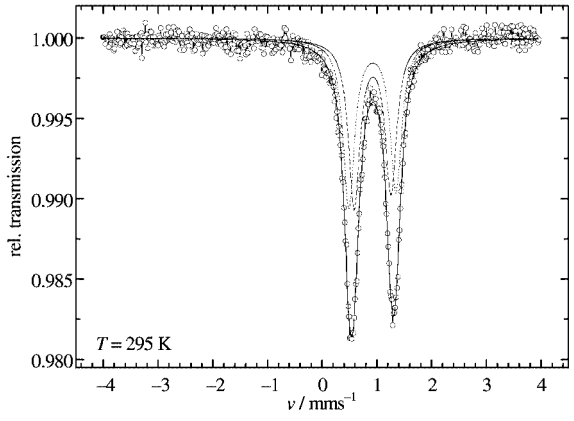


Figure 4. $^{57}$Fe Mössbauer spectra recorded from [Fe(*teef*)$_6$](BF$_4$)$_2$ at room temperature; circles depict experimental points, solid (broken) lines are computer fits as described in the text

Table 3. Isomer shift (δ) and quadrupole splitting (Δ) obtained for [Fe(*teef*)$_6$](BF$_4$)$_2$

| $T$ [K] | $A_{LS}$ [%] | $\delta_{LS}$ [mm·s$^{-1}$] | $\Delta_{LS}$ [mm·s$^{-1}$] | $A_{HS1}$ [%] | $\delta_{HS1}$ [mm·s$^{-1}$] | $\Delta_{HS1}$ [mm·s$^{-1}$] | $A_{HS2}$ [%] | $\delta_{HS2}$ [mm·s$^{-1}$] | $\Delta_{HS2}$ [mm·s$^{-1}$] |
|---|---|---|---|---|---|---|---|---|---|
| 4.2 | 56 | 0.43 | 0.13 | 21 | 1.03 | 1.54 | 21 | 1.06 | 0.98 |
| 100 | 49 | 0.41 | 0.14 | 26 | 1.02 | 1.06 | 26 | 1.01 | 0.75 |
| 110 | 46 | 0.41 | 0.14 | 27 | 1.01 | 1.07 | 27 | 1.01 | 0.75 |
| 120 | 45 | 0.41 | 0.15 | 27 | 1.00 | 1.10 | 27 | 1.01 | 0.74 |
| 130 | 41 | 0.41 | 0.12 | 29 | 1.02 | 1.14 | 29 | 1.01 | 0.78 |
| 140 | 21 | 0.33 | 0.15 | 39 | 1.06 | 1.29 | 39 | 1.01 | 0.91 |
| 150 | 7 | 0.32 | 0.18 | 47 | 1.00 | 1.38 | 47 | 0.98 | 0.94 |
| 160 | 2 | 0.32 | 0.20 | 49 | 1.00 | 1.35 | 49 | 0.98 | 0.92 |
| 170 | 0 | – | – | 50 | 0.99 | 1.31 | 50 | 0.99 | 0.86 |
| 180 | 0 | – | – | 50 | 0.99 | 1.25 | 50 | 0.99 | 0.84 |
| 190 | 0 | – | – | 50 | 0.98 | 1.22 | 50 | 0.99 | 0.80 |
| 200 | 0 | – | – | 50 | 0.97 | 1.17 | 50 | 0.97 | 0.78 |
| 295 | 0 | – | – | 50 | 0.92 | 0.86 | 50 | 0.92 | 0.68 |

  

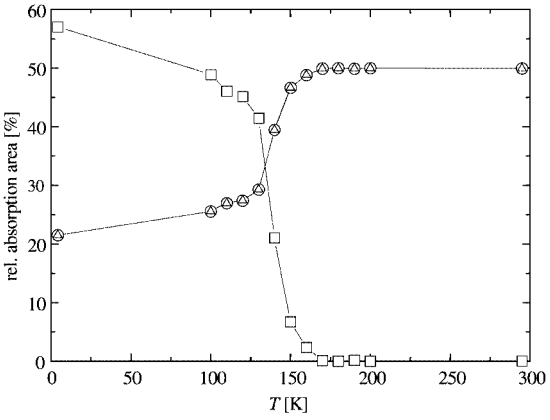


Figure 5. Relative absorption area vs. temperature derived from the $^{57}$Fe Mössbauer spectra recorded from [Fe(*teef*)$_6$](BF$_4$)$_2$ with the low-spin component (squares) and the two high-spin components (circles and triangles); the lines are merely a guide to the eye

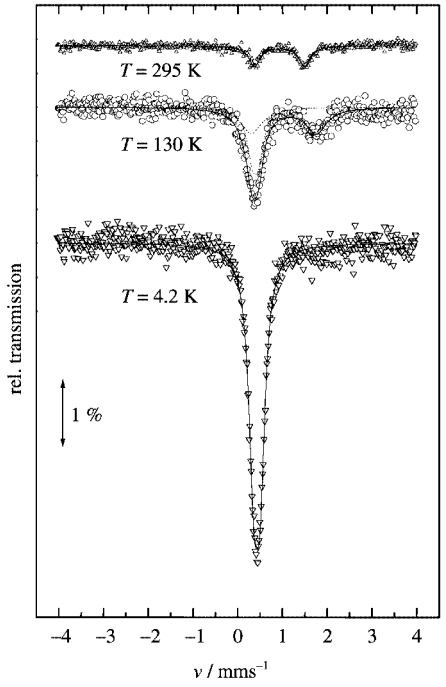


Figure 6. $^{57}$Fe Mössbauer spectra recorded from [Fe(*teeb*)$_6$](BF$_4$)$_2$ at different temperatures; triangles and circles are experimental points, solid (broken) lines are computer fits as described in the text

### *teei*

The spin transition observed from a $^{57}$Fe Mössbauer spectrum of the compound [Fe(*teei*)$_6$](BF$_4$)$_2$ (see Figure 7, Table 5) is similar to the transition in [Fe(*teeb*)$_6$](BF$_4$)$_2$. The transition is gradual and complete and occurs between 160 and approximately 250 K. Again, only one doublet, associated with iron(II) high-spin species, is detected. The transition temperature as determined by Mössbauer spectroscopy is slightly below 200 K.

Figure 8 shows the spin-transition behaviour of all three compounds as obtained from $^{57}$Fe Mössbauer spectroscopy; $\gamma_{HS}$ can be directly calculated from the peak areas of the high-spin species ($A_{HS}$) and in the case of [Fe(*teef*)$_6$](BF$_4$)$_2$ from the combination of the peak areas $A_{HS}'$ and $A_{HS}''$.

The isomer shift reflects the electron density at the Mössbauer nucleus. In the case of the high-spin state no significant influence of the individual ligand is observed. This is, however, not the case for the spectra arising from the low-spin state (Tables 3−5). The values obtained for [Fe(*teei*)$_6$](BF$_4$)$_2$ are considerably smaller than the others, indicating a larger (predominantly *s*-) electron density for this particular compound. For all three compounds under investigation the line width observed for both the high-spin and the low-spin pattern lies significantly beyond the value of the source ($> 0.3$ mm·s$^{-1}$ compared to 0.22 mm·s$^{-1}$). This might be caused by slight inhomogeneities or defects in the sample disturbing the lattice periodicity.

## Magnetic Susceptibility Measurements

In Figure 9, the fractions of the high-spin species vs. temperature (i.e. $\gamma_{HS}$ vs. $T$) of all iron(II) spin-crossover complexes studied are shown. The compounds with tetrafluoroborate as the anion are plotted in graph A, the compounds with perchlorate as the anion are plotted in graph B.

### *teef*

A significant difference is observed between the two magnetic susceptibility curves associated with the two complexes with *teef* as the ligand. The curve of the BF$_4$ complex shows a spin transition between 123 and 190 K with $T_{1/2}(1) = 137$ K and a second more gradual spin transition between 65 and 123 K with $T_{1/2}(2) = 108$ K. Each of these steps represent approximately one third of the iron(II) ions. One third of the ions do not undergo a temperature dependent spin transition, but remain in the high-spin state at all temperatures.

The curve of the magnetic susceptibility versus temperature for the perchlorate complex differs from the tetrafluoroborate complex, showing a one-step transition between 65 and 200 K with $T_{1/2} = 130$ K, thus featuring a higher spin-transition temperature than in the BF$_4$ complex. When the sample is cooled rapidly (cooling rate $>$ 50 K/min) a fraction of the iron(II) ions is trapped in the high-spin state. At approximately 55 K, this fraction transfers to the low-spin state, as depicted in Figure 9, B by a small decline of $\gamma_{HS}$ between 55 and 65 K.

### *teeb*

From magnetic susceptibility measurements of both the tetrafluoroborate and the perchlorate complexes the presence of only one magnetic site is concluded. Both compounds undergo an almost complete and gradual spin transition (over 90%) with transition temperatures of $T_{1/2} =$ 166 K for the tetrafluoroborate complex and $T_{1/2} = 150$ K for the perchlorate complex. In contrast to the *teec* com-

  

Table 4. Isomer shift (δ) and quadrupole splitting (Δ) obtained for $[Fe(teeb)_6](BF_4)_2$

| $T$ [K] | $A_{LS}$ [%] | $\delta_{LS}$ [mm·s$^{-1}$] | $\Delta_{LS}$ [mm·s$^{-1}$] | $A_{HS}$ [%] | $\delta_{HS}$ [mm·s$^{-1}$] | $\Delta_{HS}$ [mm·s$^{-1}$] |
|---|---|---|---|---|---|---|
| 4.2 | 100 | 0.43 | 0.14 | 0 | | |
| 50 | 100 | 0.44 | 0.13 | 0 | | |
| 100 | 100 | 0.43 | 0.13 | 0 | | |
| 120 | 71.6 | 0.43 | 0.13 | 20.1 | 1.09 | 1.46 |
| 130 | 77.8 | 0.44 | 0.13 | 22.2 | 1.03 | 1.60 |
| 140 | 79 | 0.43 | 0.22 | 21.0 | 1.01 | 1.53 |
| 150 | 60.5 | 0.42 | 0.14 | 39.5 | 1.04 | 1.43 |
| 160 | 45.6 | 0.40 | 0.14 | 54.4 | 1.03 | 1.45 |
| 170 | 47.1 | 0.41 | 0.15 | 52.9 | 0.97 | 1.43 |
| 180 | 32 | 0.40 | 0.13 | 68 | 1.00 | 1.33 |
| 190 | 12.9 | 0.37 | 0.13 | 87.1 | 1.02 | 1.34 |
| 200 | 15 | 0.35 | 0.13 | 85 | 0.98 | 1.30 |
| 210 | 9.5 | 0.35 | 0.13 | 90.5 | 0.97 | 1.29 |
| 220 | 0 | | | 100 | 0.98 | 1.29 |
| 295 | 0 | | | 100 | 0.92 | 1.11 |

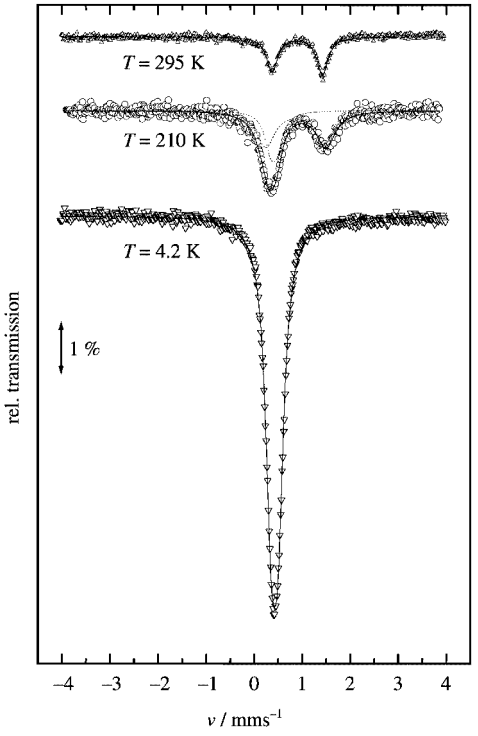


Figure 7. $^{57}$Fe Mössbauer spectra recorded from $[Fe(teei)_6](BF_4)_2$ at different temperatures; triangles and circles are experimental points, solid (broken) lines are computer fits as described in the text

plexes[8] and to $[Fe(teef)_6](BF_4)_2$ the shape of the transition curves indicates that only one Fe site is present.

***teei***

In the magnetic susceptibility data of the *teei* compounds the transition curves of both the tetrafluoroborate and the perchlorate complex show a gradual transition. The transitions are 100% complete. The curves are steeper than those of the *teeb* complexes. It is also possible that in the $[Fe(teei)_6](ClO_4)_2$ compound two different magnetic sites are present, with an "inflection point" at 167.5 K. In the first derivative of the transition curve two maxima are visible at 150 and 195 K. The overall curve appears more gradual than the curve of the tetrafluoroborate compound.

## Conclusion

In order to draw conclusions on the influence of the ligand, the results described in this paper are also compared with the equivalent *teec* complexes described previously.[8] The magnetic data of the crystallised *teec* compounds have been used for this purpose.

On summarising the two series of [(haloethyl)tetrazole]-iron(II) complexes, with $BF_4^-$ and $ClO_4^-$ as counterions several observations can be made (see Figure 9).

In both parts of Figure 9 (A and B) the sequence of the transition temperature of complexes with *teef*, *teeb* and *teei* as ligands corresponds with the size of the halogen atom. An increase in size correlates with an increase of the transition temperature. Because of the two-step transition in $[Fe(teec)_6](BF_4)_2$ and the partial transition in $[Fe(teec)_6](ClO_4)_2$ it is difficult to include these two in this order. What can be concluded is that the temperature range of the $[Fe(teec)_6](anion)_2$ samples is in the same range as that of the $[Fe(teeb)_6](anion)_2$ compounds, and between those of the *teef* and *teei* complexes.

In $[Fe(teef)_6](BF_4)_2$ a difference is observed between the spin transition obtained by Mössbauer spectroscopy and by magnetic susceptibility measurements. Both show a transition in approximately the same temperature range, but the fraction of iron(II) ions in the high-spin state at low temperature differs, with 44% high spin found by Mössbauer spectroscopy, and 35% by magnetic susceptibility. Ongoing structural measurements at low temperature will conclude whether a 1:2, or a 1:1, or no precise ratio at all, is found.[22]

Moreover, a splitting of the aromatic C−H bands in the $[Fe(teef)_6](BF_4)_2$ indicated the presence of different aromatic C−H vibrations, in other words in the same spin state, different tetrazole rings are present. Powder X-ray structure determination will have to be used to confirm whether the difference is caused by the presence of two

  

Table 5. Isomer shift (δ) and quadrupole splitting (Δ) obtained for $[Fe(teei)_6](BF_4)_2$

| $T$ [K] | $A_{LS}$ [%] | $\delta_{LS}$ [mm·s$^{-1}$] | $\Delta_{LS}$ [mm·s$^{-1}$] | $A_{HS}$ [%] | $\delta_{HS}$ [mm·s$^{-1}$] | $\Delta_{HS}$ [mm·s$^{-1}$] |
|---|---|---|---|---|---|---|
| 4.2 | 100 | 0.43 | 0.14 | 0 | | |
| 50 | 100 | 0.43 | 0.25 | 0 | | |
| 100 | 100 | 0.43 | 0.13 | 0 | | |
| 150 | 100 | 0.42 | 0.17 | 0 | | |
| 160 | 100 | 0.40 | 0.18 | 0 | | |
| 170 | 92.5 | 0.40 | 0.28 | 7.5 | 0.87 | 1.57 |
| 180 | 87.7 | 0.41 | 0.40 | 12.3 | 0.86 | 1.67 |
| 190 | 61.2 | 0.37 | 0.31 | 38.8 | 0.88 | 1.30 |
| 200 | 48.6 | 0.42 | 0.21 | 51.4 | 0.89 | 1.35 |
| 210 | 38.4 | 0.41 | 0.14 | 61.6 | 0.87 | 1.26 |
| 220 | 38.0 | 0.34 | 0.21 | 62.0 | 0.92 | 1.13 |
| 230 | 25.6 | 0.31 | 0.20 | 74.4 | 0.97 | 1.14 |
| 240 | 9.7 | 0.33 | 0.21 | 90.3 | 0.95 | 1.13 |
| 295 | 0 | | | 100 | 1.05 | 1.20 |

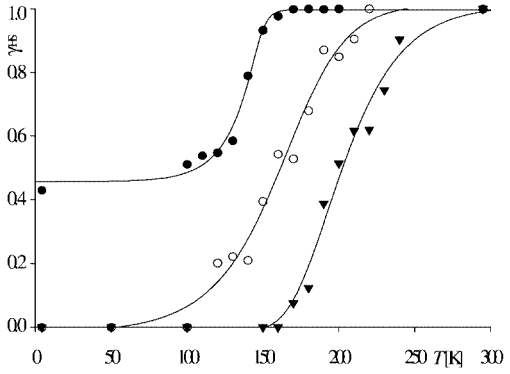


Figure 8. $\gamma_{HS}$ (directly calculated from the relative absorption area of the high-spin species) vs. temperature derived from the $^{57}$Fe Mössbauer spectra recorded from $[Fe(teef)_6](BF_4)$ (dots), $[Fe(teeb)_6](BF_4)$ (circles) and $[Fe(teei)_6](BF_4)_2$ (triangles); the sigmoidal lines are merely a guide to the eye

symmetrically non-equivalent tetrazole rings coordinated to the same iron(II) ion, or by two symmetrically non-equivalent iron(II) species. The last option is supported by the magnetic data and is proved independently by $^{57}$Fe Mössbauer spectroscopy. In either case, the vibrational spectrum not only gives qualitative information about the spin-transition temperature $T_{1/2}$, but also about structural properties. This opens additional possibilities for the use of variable-temperature IR spectroscopy as a tool in the investigation of spin-crossover compounds.

The complexes with *teec* as ligand, $[Fe(teef)_6](BF_4)_2$ and $[Fe(teei)_6](ClO_4)_2$ all show a complicated spin-crossover behaviour, perhaps with the presence of two (or in the case of *teef* possibly even three) different sites. This spin-crossover behaviour is simpler in both the *teeb* compounds, perchlorate complex with *teef* ligands and the tetrafluoroborate complex with *teei* ligands, which all show gradual transitions without any steps.

Only in the complexes with *teeb* as the ligand is the influence of the counterion small (only a difference in transition temperature). In all other compounds the magnetic behaviour varies strongly from the tetrafluoroborate to the perchlorate complex. In the *teeb* complexes alone the transition curves shift to a slightly lower temperature when tetrafluoroborate is replaced by perchlorate. This behaviour has been observed before in mononuclear spin-crossover complexes.[23]

Structural analyses indicate that all compounds crystallise as iron(II) complexes with six (haloethyl)tetrazole ligands octahedrally surrounding each iron(II) centre.[22] At

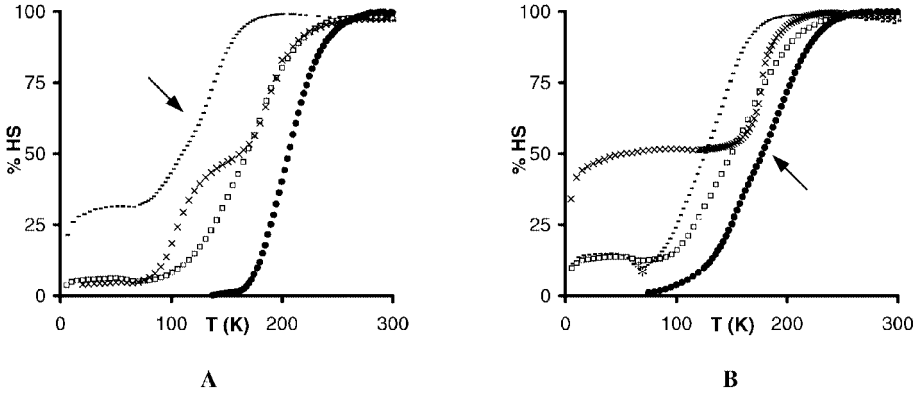


Figure 9. Transition curves of $[Fe(teex)_6](anion)_2$ with *teex* = *teef* (—), *teec* (×), *teeb* (squares), *teei* (dots); A) anion = $BF_4^-$, B) anion = $ClO_4^-$ (for *teex* = *teec*, curves of the crystallised samples[8] are depicted); the arrows indicate the "bend" between two possible different transition curves, the * indicates the small step caused by thermal trapping in $[Fe(teef)_6](ClO_4)_2$

  

room temperature, all compounds studied by powder XRD appear to be isostructural to $[Fe(teec)_6](BF_4)_2$, with space group $P2_1/c$,[22] except for $[Fe(teef)_6](BF_4)_2$, which is triclinic in structure instead of monoclinic. Further studies will indicate whether or not the complex spin transition is caused by structural or thermodynamic properties.[22]

Variable-temperature mid-range infrared spectroscopy has been applied to supplement data obtained by magnetic susceptibility measurements and Mössbauer spectroscopy. As shown by a comparison of the spectra of the free ligands and the respective complexes, band shifts are indeed seen to originate from the different substituents used. But the thermally induced spin transition of the iron(II) coordination centres definitely has the strongest impact on the vibrational spectra. The direct observation of the bond-strength changes of the Fe−N bonds upon spin transition in the far IR region turns out to be difficult, mainly because of the coupling of intra-ligand vibrational modes with the Fe−N stretching vibration. Nevertheless, an indirect monitoring of the Fe−N bond strength changes can be achieved by variable-temperature mid-range IR spectroscopy. The focus of interest is the stretching vibration of the single hydrogen atom on the tetrazole ring. This aromatic C−H vibration can easily be distinguished from the aliphatic C−H vibrations of the alkyl substituents. It does not couple with other vibrations and is reasonably sensitive to the bond-strength change of the neighbouring Fe−N bond. Thus, with variable-temperature IR as a tool, it is possible to monitor the spin transition (in this case qualitative, but in other cases quantitative). In the case of a reasonably large band shift of this C−H band, which depends on the packing of the complex, a quantification of the respective peak intensities allows an independent determination of $T_{1/2}$.[23]

The influence of the substituent of the ethyl tail on the electron density of the tetrazole is virtually nonexistent. Therefore, the differences in the spin-transition behaviour should be caused entirely by the crystal packing. The iron−iron distance, and thereby the strength of the elastic interaction (larger when the relative volume change is larger), as well as the relative size of the anion compared to the cationic centre, seem to be the most important causes for the differences in the spin-transition behaviour. But no correlation has been observed between spin transition (i.e. $\gamma_{HS}$ vs. $T$) on the one hand, and space group, anion and ligand size on the other. Therefore, it is not yet possible to predict the magnetic properties of a new spin-crossover compound with 1-alkyltetrazoles as ligands.

## Experimental Section

**General Remarks:** Vibrational spectra were recorded with a Perkin−Elmer 16 PC mid-range FT-IR spectrometer using a Graseby-Specac thermostattable sample holder with a Graseby-Specac automatic temperature controller within the temperature range of 100−300 K. To accomplish a reasonable signal-to-noise ratio 64 scans have been summed. Magnetic susceptibility measurements (5−300 K) were carried out using a Quantum Design MPMS-5 5T SQUID magnetometer (measurements carried out at 0.1 T). The data were corrected for the magnetisation of the sample holder and for diamagnetic contributions, which were estimated from the Pascal constants.[25] C,H,N determinations were performed with a Perkin−Elmer 2400 Series II analyser. The $^{57}$Fe Mössbauer spectra were recorded between 4.2 and 295 K using a conventional constant acceleration drive system. The source used was $^{57}$Co in an Rh matrix with an activity of about 50 mCi. The data were analysed using a least-squares fitting program package under the assumption of a discrete superposition of Lorentzian lines. Since the high-spin and the low-spin pattern overlap to a certain extent, the errors of the hyperfine parameters, determined from the computer fit, i.e. isomer shift and quadrupole splitting, increase with decreasing absorption area of the given sub-spectrum from ± 0.01 mm·s$^{-1}$ above 20% area to 0.05 mm·s$^{-1}$ for an area of the order of a few percent. The isomer-shift values displayed in the tables are given relative to the source. If the values are to be compared with shifts relative to α-Fe, 0.12 mm·s$^{-1}$ have to be added.

**2-(1-Fluoroethyl)tetrazole (*teef*):** This compound was obtained by refluxing a mixture of (1-fluoroethyl)amine hydrochloride (0.05 mol, 5.0 g) and sodium azide (0.01 mol, 6.5 g) in acetic acid (30 mL) and triethyl orthoformate (60 mL) for 8 h. The excess solvents were removed by evaporation. The product was extracted by treating the residue with 2-propanol and removing the insoluble salts (sodium chloride and unchanged sodium azide) by filtration. After further evaporation of the solvent, a yellow oil remained. The pure ligand was obtained by placing the $[Cu(teef)_2Br_2]_n$ complex in ethanol, dissolving this complex in water and extracting the *teef* ligand with dichloromethane. The yield is approximately 1.2 g (20%). $^1$H NMR (300 MHz, [D$_6$]DMSO): δ = 9.39 (s, CH), 4.88 (t, CH$_2$), 3.77 (t, CH$_2$) ppm. $^{13}$C NMR (75 MHz, [D$_6$]DMSO): δ = 144.5 (CH), 48.7 (CH$_2$), 48.4 (CH$_2$) ppm.

**2-(1-Bromoethyl)tetrazole (*teeb*):** This compound was obtained by refluxing a mixture of (1-bromoethyl)amine hydrobromide (0.25 mol, 51 g) and sodium azide (0.3 mol, 22 g) in acetic acid (100 mL) and triethyl orthoformate (200 mL) for 6 h. After evaporation of the excess solvents and removal of the salts formed by filtration, the yellow oil obtained was dissolved in 2-propanol. After another subsequent filtration to remove the insoluble salts, *teeb* crystallised as a white solid after several weeks. The yield was approximately 0.9 g (20%). $C_3H_5BrN_4$ (177.0): calcd. C 20.4, H 3.0, N 31.7; found C 21.4, H 2.9, N 33.7. $^1$H NMR (300 MHz, [D$_6$]DMSO): δ = 9.47 (s, CH), 4.92 (t, CH$_2$), 3.98 (t, CH$_2$) ppm. $^{13}$C NMR (75 MHz, [D$_6$]DMSO): δ = 144.4 (CH), 49.2 (CH$_2$), 42.8 (CH$_2$) ppm.

**2-(1-Iodoethyl)tetrazole (*teei*):** This compound was synthesised according to the Finkelstein reaction,[26,27] which involves substitution, starting from 2-(1-bromoethyl)tetrazole (*teeb*) and sodium iodide (1.5 equiv.). A 10% solution of *teeb* and sodium iodide in acetone was stirred under reflux conditions for over 2 h. At this stage, the bromide was substituted for iodide and the insoluble sodium bromide precipitated. After cooling, the solution was filtered to remove the insoluble sodium bromide and after removal of the solvent, the remaining oil was dissolved in water; *teei* was obtained by extraction with chloroform after removal of the solvent. The oil obtained slowly crystallised from 2-propanol. The yield was approximately 1 g (60%). $^1$H NMR (250 MHz, [D$_6$]DMSO): δ = 9.45 (s, CH), 4.82 (t, CH$_2$), 3.66 (t, CH$_2$) ppm. $^{13}$C NMR (68 MHz, [D$_6$]DMSO): δ = 144.4 (CH), 49.9 (CH$_2$), 3.26 (CH$_2$) ppm.

***WARNING:** Perchlorate salts are potentially explosive and when used should be treated as such!*

**$[Fe(teef)_6](BF_4)_2$:** This complex was prepared by dissolving $Fe(BF_4)_2{\cdot}6H_2O$ (1.0 mmol, 0.30 g) and *teef* (6.0 mmol, 0.70 g) in

  

ethanol (20 mL). The complex formed as white hexagonal-shaped crystallites, yield 90 mg (10%). $C_{18}H_{30}B_2F_{14}FeN_{24}$ (926.0): calcd. C 23.3, H 3.3, N 36.3; found: C 23.1, H 2.6, N 36.7.

**[Fe(*teef*)$_6$](ClO$_4$)$_2$:** This complex was formed by dissolving $Fe(ClO_4)\cdot 6H_2O$ (1.0 mmol, 0.36 g) and *teef* (6.0 mmol, 0.70 g) in ethanol (20 mL). The complex formed as white hexagonal-shaped crystallites, yield 140 mg (15%). $C_{18}H_{30}Cl_2F_6FeN_{24}O_8$ (951.3): calcd. C 22.7, H 3.2, N 35.3; found C 22.5, H 2.8, N 35.6.

**[Fe(*teeb*)$_6$](BF$_4$)$_2$:** This complex was formed by dissolving $Fe(BF_4)_2\cdot 6H_2O$ (1.0 mmol, 0.30 g) and *teeb* (0.6 mmol, 1.06 g) in ethanol (40 mL). The complex formed as white hexagonal-shaped crystallites, yield 240 mg (20%). $C_{18}H_{30}B_2Br_6F_8FeN_{24}$ (1291.5): calcd. C 16.7, H 2.3, N 26.0; found C 18.0, H 2.6, N 25.6.

**[Fe(*teeb*)$_6$](ClO$_4$)$_2$:** This complex was formed by dissolving $Fe(BF_4)_2\cdot 6H_2O$ (1.0 mmol, 0.30 g) and *teeb* (6.0 mmol, 1.06 g) in ethanol (40 mL). The complex formed as white hexagonal-shaped crystallites, yield 250 mg (20%). $C_{18}H_{30}Br_6Cl_2FeN_{24}O_8$ (1316.8): calcd. C 16.4, H 2.3, N 25.5; found C 17.5, H 2.7, N 24.9.

**[Fe(*teei*)$_6$](BF$_4$)$_2$:** This complex was formed by dissolving $Fe(BF_4)_2\cdot 6H_2O$ (1.0 mmol, 0.30 g) and *teei* (6.0 mmol, 1.34 g) in ethanol (40 mL). The complex formed as white hexagonal-shaped crystallites, yield 0.7 g (45%). $C_{18}H_{30}B_2F_8FeI_6N_{24}$ (1573.5): calcd. C 13.7, H 1.9, N 21.4; found C 13.8, H 1.9, N 21.5.

**[Fe(*teei*)$_6$](ClO$_4$)$_2$:** This complex was formed by dissolving $Fe(ClO_4)\cdot 6H_2O$ (1.0 mmol, 0.36 g) and *teei* (6.0 mmol, 1.34 g) in ethanol (40 mL). The complex formed as white hexagonal-shaped crystallites, yield 0.8 g (50%). $C_{18}H_{30}Cl_2FeI_6N_{24}O_8$ (1598.8): calcd. C 13.5, H 1.9, N 21.0; found for C 13.7, H 1.5, N 20.7.

## Acknowledgments

Thanks for financial support go to the "Fonds zur Förderung der Wissenschaftlichen Forschung in Österreich" (Project 15874-N03), the Training and Mobility of Researchers Network (TMR) project "Thermal and Optical Spin State Switching" (TOSS) supported by the European Community under the Contract number ERB-FMRX-CT98-0199 and to the European Science Foundation under the project "Molecular Magnets". Jos van Brussel is acknowledged for the elemental analyses. The work described in this paper has been supported by the Leiden University Study group WFMO and has been performed under the auspices of the Graduate Research School HRSMC, a joint activity of Leiden University and the two Universities in Amsterdam.

[1] J. Jeftic, R. Hinek, S. C. Capelli, A. Hauser, *Inorg. Chem.* **1997**, 3080−3087.
[2] P. L. Franke, J. G. Haasnoot, A. P. Zuur, *Inorg. Chim. Acta* **1982**, 5−9.
[3] P. Gütlich, P. Poganiuch, *Angew. Chem. Int. Ed. Engl.* **1991**, 975−977.
[4] T. Buchen, P. Gütlich, *Chem. Phys. Lett.* **1994**, 262−266.
[5] A. Hauser, P. Gütlich, H. Spiering, *Inorg. Chem.* **1986**, 4245−4248.
[6] N. Willenbacher, H. Spiering, *J. Phys. Chem. Solid State Phys.* **1988**, *21*, 1423.
[7] P. Poganiuch, P. Gütlich, *Hyperfine Interact.* **1988**, 331−334.
[8] A. F. Stassen, E. Dova, J. Ensling, H. Schenk, P. Gütlich, J. G. Haasnoot, J. Reedijk, *Inorg. Chim. Acta* **2002**, 61−68.
[9] A. Camard, M. Grunert, W. Linert, unpublished results.
[10] A. F. Stassen, PhD Thesis, Leiden University, Leiden, The Netherlands, **2002**.
[11] M. Hesse, H. Meyer, B. Zeeh, *Spektroskopische Methoden in der Organischen Chemie*, 5th ed., Thieme Verlag, Stuttgart, **1995**.
[12] E. Lieber, D. R. Levering, L. J. Patterson, *Anal. Chem.* **1951**, *11*, 1594−1604.
[13] F. Billes, H. Endrédi, G. Keresztury, *THEOCHEM* **2000**, 183−200.
[14] S. C. S. Bugalho, E. M. S. Maçôas, M. L. S. Cristiano, R. Fausto, *Phys. Chem.* **2001**, 3541−3547.
[15] R. D. Holm, P. L. Donnelly, *J. Inorg. Nucl. Chem.* **1966**, *1887−1894*.
[16] E. O. J. John, R. D. Willet, B. Scott, R. L. Kirchmeier, J. M. Shreeve, *Inorg. Chem.* **1989**, 893−897.
[17] H. B. Jonassen, J. O. Terry, A. D. Harris, *J. Inorg. Nucl. Chem.* **1963**, 1239−1243.
[18] K. Nakamoto, *Infrared and Raman Spectra of Inorganic and Coordination Compounds*, 4th ed., ISBN 0-471-01066-9, John Wiley & Sons, New York, **1986**.
[19] J. Schweifer, P. Weinberger, K. Mereiter, M. Boca, C. Reichl, G. Wiesinger, G. Hilscher, P. J. v. Koningsbruggen, H. Kooijman, M. Grunert, W. Linert, *Inorg. Chim. Acta* **2002**, 297−306.
[20] P. Gütlich, A. Hauser, H. Spiering, *Angew. Chem. Int. Ed. Engl.* **1994**, 2024−2054.
[21] R. A. Nyquist, C. L. Putzig, M. A. Leuger, *Infrared and Raman Spectral Atlas of Inorganic Compounds and Organic Salts*, vols. 1, 3 and 4, Academic Press, **1996**.
[22] E. Dova, A. F. Stassen, M. Grunert, R. Peschar, J. G. Haasnoot, W. Linert, J. Reedijk, H. Schenk, manuscript to be submitted.
[23] L. Wiehl, *Acta Crystallogr., Sect. B* **1993**, 289−303.
[24] P. J. van Koningsbruggen, M. Grunert, P. Weinberger, *Monatsh. Chem.* **2003**, *134*, 183−198.
[25] I. M. Kolthoff, P. J. Elving, *Treatise on Analytical Chemistry*, vol. 4, New York, **1963**.
[26] A. Roedig, *Methoden Org. Chem (Houben-Weyl)* **1960**, vol. 4/5, pp. 595−605.
[27] J. A. Miller, M. J. Nunn, *J. Chem. Soc., Perkin Trans. 1* **1976**, 416.

Received November 27, 2002

  